Proceedings 10th NUMGE 2023
10th European Conference on Numerical Methods in Geotechnical Engineering
Zdravkovic L, Kontoe S, Taborda DMG, Tsiampousi A (eds)

https://doi.org/10.53243/NUMGE2023-263

Correlation analysis of the hypoplastic clay parameters based on ExCalibre dataset database

P.C. Do[1] , T. Kadlíček[1] , D. Mašín[1], J. Najser[1]

[1]*Institute of Hydrogeology, Engineering Geology and Applied Geophysics, Charles University, Czech Republic*

ABSTRACT: The ExCalibre, which was developed as an online calibration software, has found its place in the scientific and engineering community. The application currently supports calibration for four constitutive models, hypoplastic clay, hypoplastic sand, Modified Cam-Clay and Mohr-Coulomb models. To initiate a calibration, the software requires input of laboratory data in the form of Excel file whose template is available on the website of ExCalibre software. In addition, the data must include a combination of compression and shear test results. During the recent years of software operation, the users uploaded a number of laboratory data spreadsheets, which can be (by the software licence agreement) used anonymously by software developers for research purposes. This database currently includes over 200 unique specimens which are here analysed in order to deduce correlations between the constitutive models parameters and soils index characteristics. These relations can serve for prompt preliminary evaluation of the constitutive models parameters, thereby promoting the advancement of constitutive models in both fields of practice and science.

Keywords: Hypoplastic clay; ExCalibre; correlation analysis

1 INTRODUCTION

Over the decades, researchers have been dedicated to predict the soil behaviours under various conditions by introducing more advanced constitutive theories. Although these models have their advantages in simulating and predicting stresses and displacements of soil under varied conditions, the practical applications of these models are far from the desired level. This state is mainly due to the complexity of implementing advanced models into finite element codes, and challenging calibration procedure of constitutive model parameters, which often requires several cycles of back calculation on available laboratory experiments.

For the latter reason, correlation analyses can serve as a practical tool for a prompt estimation of model parameters in cases of simple geotechnical conditions. Correlation provides mathematical relationships, as a preliminary approximation to a particular parameter, often based on other commonly measured soil properties such as Atterberg's limits or particle size distribution.

In this paper, correlation relations are deduced between the parameters of the hypoplastic clay model (Mašín, 2014) which is implemented in the ExCalibre software (Kadlíček et al., 2022a, 2022b), and soil properties. The ExCalibre input data are stored (according to the software licence agreement) for later anonymous analyses and contains both compression (isotropic and oedometric) and triaxial (drained and undrained) experiments. Since the launch of ExCalibre, more than 2000 individual input files have been stored and after close inspection over 200 were identified as unique, not faulty, and suitable for further analyses.

First, the model formulation and its five parameters will be briefly described. Subsequently, descriptions of tests data which were used for calibration with the ExCalibre will be provided. Eventually, results and correlation analyses for each parameter are presented.

2 HYPOPLASTIC CLAY

The model introduced in Mašín (2014), is developed based on the hypoplastic clay model developed in Mašín (2013). It defines the asymptotic state boundary surface in space of stress and void ratio, encompassing all admissible states. The rate formulation can be written as:

$$\dot{\sigma}_{ij} = f_s L_{ijkl}\dot{\varepsilon}_{kl} + \frac{f_d}{f_d^A} A_{ijkl} d_{kl}\sqrt{\dot{\varepsilon}_{kl}\dot{\varepsilon}_{kl}}, \qquad (1)$$

where $\dot{\sigma}_{ij}$, $\dot{\varepsilon}_{kl}$ are the stress rate and strain rate, and L_{ijkl} represents the fourth-order stiffness tensor. The scalar functions barotropy f_s and pyknotropy f_d amplify effect of stress level and density in the differential equation.

The corresponding asymptotic states are defined by the fourth-order tensor A_{ijkl} and pyknotropy at the asymptotic state, denoted as f_d^A. The second order tensor d_{kl} represents the asymptotic strain rate direction.

The hypoplastic clay model defines five parameters,

which are close in nature to those defined by the Cam-Clay model:

- λ^* – slope of the normal compression line in $\ln(e+1) \times \ln p$ plane.
- κ^*– slope of the swelling line in $\ln(e+1) \times \ln p$ plane at the isotropic state
- N – defines the position of the isotropic normal compression line in $\ln(e+1) \times \ln p$ plane at 1 kPa.
- φ_c – the critical friction angle
- ν – the parameter controlling bulk and shear modulus stiffnesses ratio

For the sake of clarity, the parameters λ^*, κ^* and N are displayed in Figure 1.

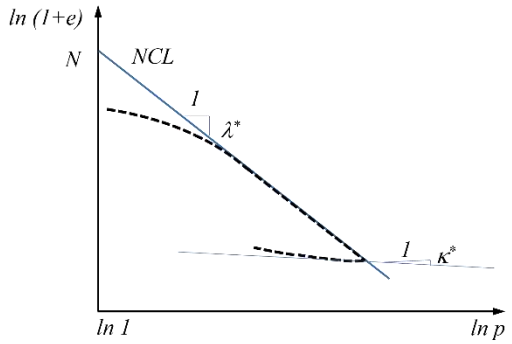

Figure 1: The parameters λ^*, κ^* N in $\ln(e+1) \times \ln p$ plane

Unlike elastoplaticity, the hypoplasticity does not utilize a Heaviside function to differentiate between the elastic and plastic mode of loading. Instead, its nonlinear behaviour is governed by a single differential tensor function.

3 DATA SAMPLES

For the preliminary analysis, a total number of 33 individual input files were used. To ensure a high level of consistency, we only selected input data that included reconstituted oedometric test (OED-REC) and two to four undrained triaxial compression tests of reconstituted nature (CIUP-REC).

Since the parameters N and λ^* control the position and the slope of the Isotropic Normal Compression Line (INCL), they control position of the asymptotic states. These states are eventually reached during a continuous proportional loading. However, it is important to note that the INCL is not typically reached in compression tests conducted on overconsolidated specimens. Consequently, the parameters N and λ^* should be calibrated and analysed based on the OED-REC specimens. Similarly, the parameter κ^* is defined as the slope of the swelling line at the isotropic state. Therefore, normally consolidated specimens OED-REC should be used for its evaluation.

The critical friction angle φ_c should be preferably determined from the CIUP-REC regardless of whether the specimens are reconstituted (REC) or undisturbed (NAT). This ensures more accurate estimation of the critical state friction angle φ_c.

While the reconstituted sample are advantageous for determining the asymptoticity driving parameters, the natural specimens (CIUP-NAT) are essential for evaluating the stiffness controlling parameter ν. Similarly, κ^* should preferably be calibrated with the use of undisturbed oedometric (OED-NAT) experiments.

The majority of soil samples in this study are classified as CL and CH according to the USCS classification. There are also 3 SC samples, one SM sample, and 4 samples classified as MH soil. The samples have a wide range of plasticity index (5% - 68%) and liquid limit (19.7% - 98%). Additionally, most of the soils have more than 50% of fine grains (< 0.063 mm).

4 CORRELATION ANALYSES

The Hypoplastic clay parameters were calibrated using the online automatic calibration tool ExCalibre (Kadlíček et al.,2022a, 2022b). Each parameter is analysed to explore its relationship with other model parameters and soil properties, such as the Atterberg's limit or particle size distribution characteristics.

The observed ranges of models parameters with their means (μ) and deviations (σ) are displayed in Table 1. Note that all parameters are unitless, except of the critical friction angle φ_c.

Table 1: Descriptions of calibrated parameters

Parameters	Range	μ (σ)
N [-]	0.501 – 1.607	0.9242 (0.234)
λ^*[-]	0.033 – 0.1358	0.0676 (0.021)
κ^*[-]	0.005 – 0.0405	0.0114 (0.007)
φ_c [°]	18.9 – 36.8	28.2 (4.4)
ν [-]	0.01 – 0.43	0.2056 (0.117)

4.1 Analysis for N and λ^*

The parameter N controls the position of the Isotropic Compression Line (INCL) in the $\ln(1+e) \times \ln p$ plane, as depicted in Figure 1. On the other hand, the parameter λ^* controlls slope of any NCL in $\ln(1+e) \times \ln p$ plane, including the slope of the critical state line (CSL). These parameters can be considered counterparts of initial void ratio e_0 and compression index C_c, which are determined from the $e_0 \times \log p$ plane. Correlations between these parameters have been reported in the literature, such as Hong et al. (2012) and they can provide valuable insights for understanding the correlation between the parameters N and λ^*. The correlation shown in Figure 2 accounts for different types of soil including Silt-

mixtures (SM), Clayed sands (SC), Silty clay (CL), Inorganic silts (MH) and high plasticity Clay (CH), yielding high correlation coefficient of $r = 0.944$.

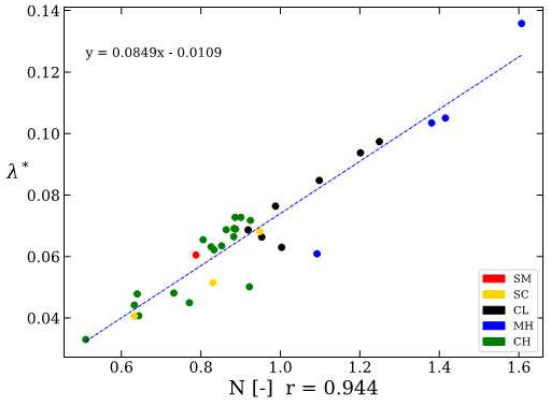

Figure 2: Correlation between N and λ^*

The positive correlation observed in the relation between parameters N and λ^* aligns with the existing literature on the correlation between the compression index (C_c) and void ratio e_0. It is widely recognized that the compression index C_c can be well-correlated to the Atterberg's limits. This stems from two assumptions:

First, the compression index is identical for NCL and CSL. Second, the undrained strength at the liquid limit W_L and at the plastic limit W_P corresponds to two different states at CSL whose slope is given by C_C (Wroth, 1978).

Interestingly, the positive relation in Figure 2 shows evidence for the Ω-points principle, which states that there is a presumed convergence point of all CSL lines, acorrding to Schofield & Wroth, (1968). The authors claim with experiments that for many fine grained soils, their CSL lines pass through an omega point, with coordinates $e_\Omega = 0.25$ and $\sigma'_\Omega = 15$ MPa.

Figure 3 shows the correlation between the two parameters and Atterberg's limits. Overall, the graphs show that the two parameters are well-correlated with the Atterberg's limits. The Pearson coefficient between λ^* and Plastic Limit is $r = 0.797$ and its value between λ^* and Liquid Limit is $r = 0.668$, as shown in Figure 3(a) and (b). The parameter N yields similar results with the Pearson coefficient $r = 0.788$ between N and W_L, and $r = 0.88$ between N and W_P. Although there exists some distant points to the regression line, these graphs show high positive correlations.

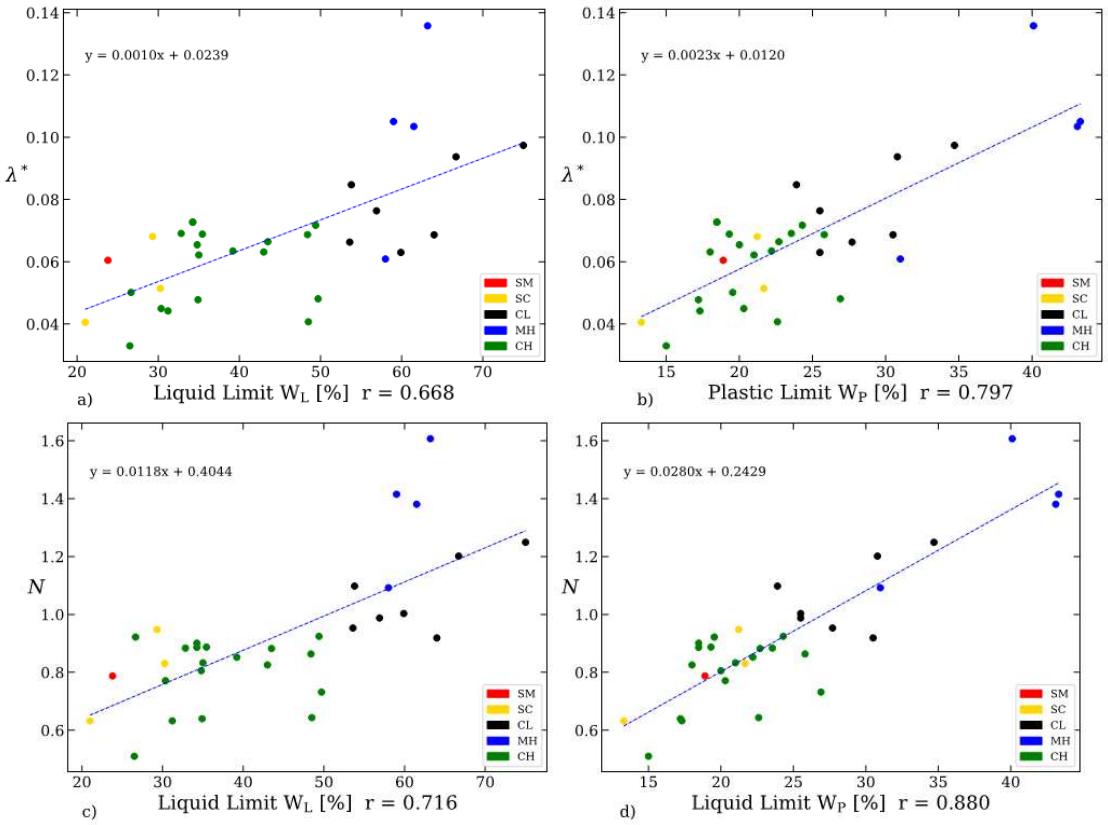

Figure 3:Relation between parameters N and λ^*, and soil Atterberg's limits with the correlation coefficient r

4.2 Analysis for κ^*

The parameter κ^* controls the slope of the isotropic unloading line in the $\ln(1+e) \times \ln p$ slane, as shown in Figure 1. Hence, this parameter holds a similar meaning to the swelling index C_s. It is recognized that C_s has a positive relation with the compression index C_c (Binod & Beena, 2011).

Therefore, it is expected that κ^* will have relations with λ^*, and N since N and λ^* are strongly related.

Figure 4(a) and (b) show the relation between $\kappa^*$and λ^* and N. The Pearson coefficients are 0.854 for $\kappa^*$and λ^*, while this value is 0.813 for $\kappa^*$and N. There is, however, a distant point, from the CL soil class, which has the highest values for both κ^*, λ^* and N.

There are clear positive trends observed. These relations also suggest that κ^* can be correlated to the Atterberg's limits, as these properties have strong correlation to λ^* and N, as shown in the previous section.

The correlation coefficient for κ^* and W_L is 0.6, while this value for κ^* and W_P is 0.657. Although these values are not too high, they show a strong relation with most data points located around the trendline, and only a distant point of CL soil which intensively skews the relation, as seen in Figure 4(c) and (d).

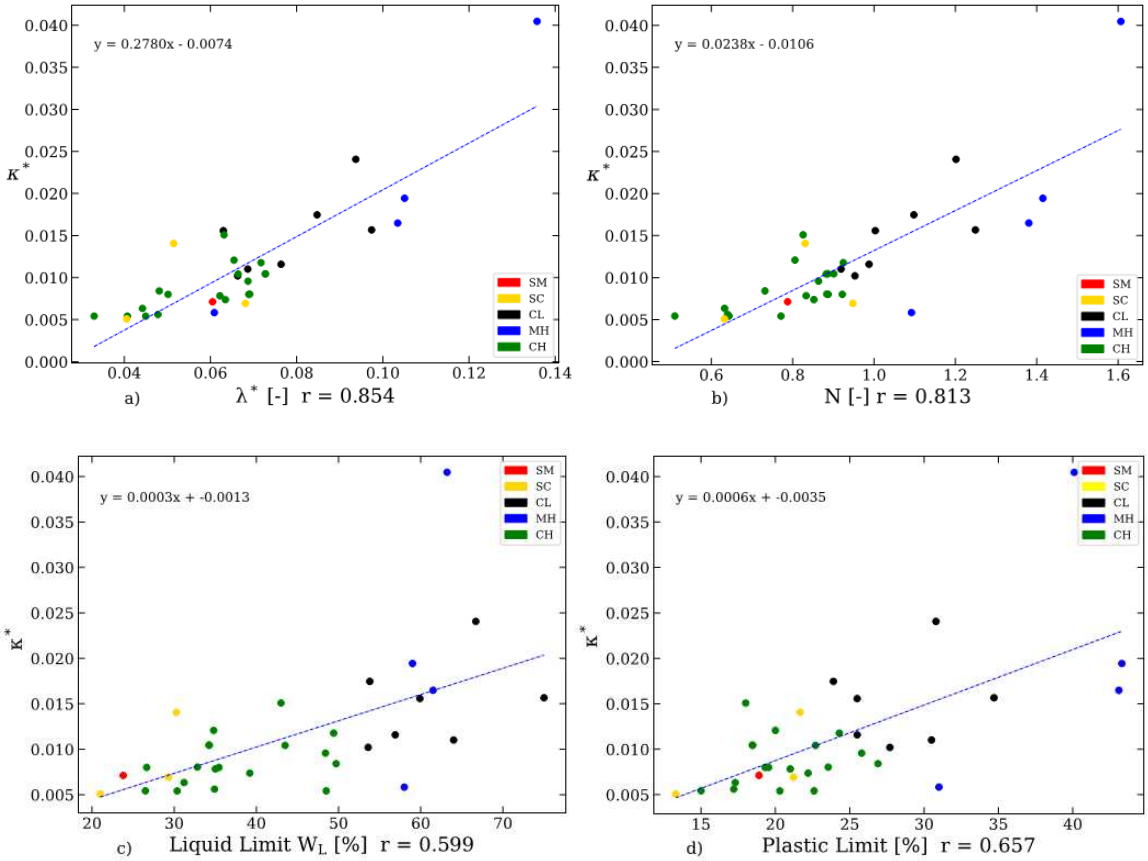

Figure 4: Relation between parameters κ^*, N and λ^*, and soil Atterberg's limits with the correlation coefficient r

4.3 Critical friction angle φ_c

Number of studies have proved that the critical friction angle has close relations with the grain size distribution. An increase of the clay fraction content 20% to 40% leads to a significant decrease in the value of the critical state friction angle (Lupini et al., 1981) .

As mentioned earlier, the liquid limit W_L and the plastic limit W_P are related to the undrained shear strength as reported by Wroth (1978) and Sharma & Bora (2003). It is postulated that the undrained shear strength of a soil at W_L and W_P corresponds to 1.7 kPa and 170 kPa, respectively.

The correlations in Table 2 display relations between the critical state friction angle φ_c and Atterberg's limits, sand (< 2 mm), fine (< 0.063 mm) and clay mineral (< 0.002) particles content.

Table 2: Correlation matrix for φ_c

W_L	W_P	I_P	< 0.063	< 2	< 0.002
-0.75	-0.67	-0.63	-0.80	0.84	-0.75

The critical strength exhibits a good correlation with grain distribution. In particular, the negative correlations with fine particles of $r = -0.80$ and clay particles of $r = -0.72$, and positive correlation with sand particles of $r = 0.84$ are in a good agreement with expectation. The correlation representation between the critical angle and the sand particle is shown in Figure 5.

The Atterberg's limits W_L, W_P show a negative correlation to the critical state friction angle, with $r = -0.75$ and $r = -0.67$, respectively. The graphical representation of the linear correlation between φ_c and Liquid Limit is illustrated in Figure 6. The negative relation between φ_c and W_P is not strong and it suggests that the linear regression is unable to describe comprehensively these parameters' relation.

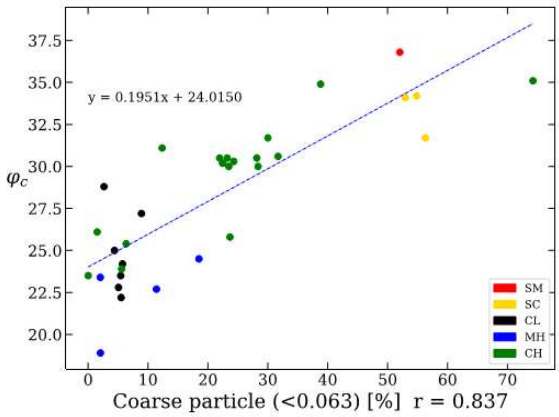

Figure 5: Correlation between φ_c and coarse particles

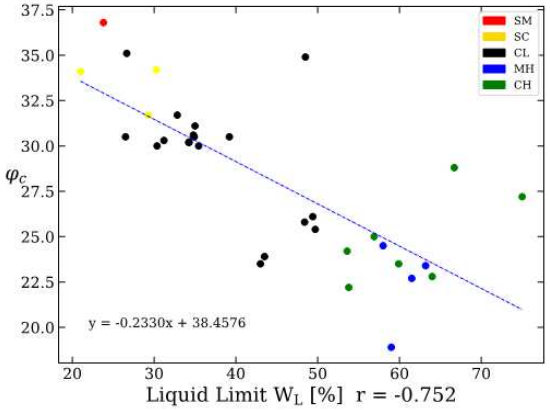

Figure 6: Correlation between φ_c and liquid limit

4.4 Analysis of the parameter ν

The parameter ν governs the relation between the bulk modulus K_i and the shear modulus G_i at the isotropic state and with the aid of the parameters λ^* and κ^* can be expressed as:

$$\nu = \frac{3\frac{K_i}{G_i}(\lambda^*+\kappa^*)-4\kappa^*}{6\frac{K_i}{G_i}(\lambda^*+\kappa^*)+4\kappa^*}. \quad (2)$$

Although the parameter controls the stiffness of the hypoplastic clay model, it cannot be directly evaluated from the stress-strain curve. Therefore, the parametric study involving element test simulation of the triaxial test is needed to fit this parameter. The meaning of the parameter ν can be derived from the graphical representation of the hypoplastic clay model's stiffness in the form of the so-called response envelope (Gudehus & Mašín, 2009), which in this case is represented with an ellipse, as displayed in Figure 7.

The aspect ratio of the ellipse (ratio between the isotropic path I_1I_2 and constant-volumetric strain path C_1C_2) is directly controlled by the parameter *ν as*:

$$\frac{|C_1C_2|}{|I_1I_2|} = \frac{1-2\nu}{1+\nu}. \quad (3)$$

Consequence of Eq. (3) is the widening of the response envelope and thus increasing the shear stiffness with decreasing ν.

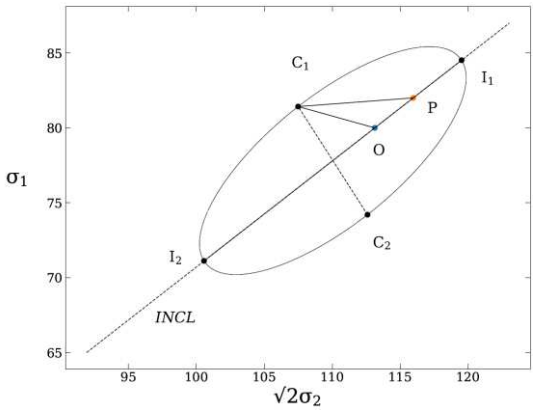

Figure 7: Response envelope in the stress space. O – current stress state, OI_2 – isotropic unloading, OI_1 – isotropic loading, OC_1– undrained triaxial compression, OC_2 undrained triaxial extension. P – isotropically normally consolidated state

Calibration of multiple input data files in the software ExCalibre revealed a trend in calibration output regarding the overconsolidation (OCR) of the specimens. To properly analyse ν, the input data protocols were split into separate files consisting of one OED-REC and one CIUP-REC test. This process created 123 separate protocols for the calibration ν at various states.

Although the parameter ν itself does not have a clear relationship towards Atterberg limits or grain size distribution, its effect on the undrained shear stiffness was observed. The calibrated undrained shear stiffness of the hypoplastic clay model at the normally consolidated state, expressed as the length $|C_1P|$, was correlated with the parameter λ^*. Since the parameter λ^* well correlates with other soil properties such as Atterberg's limits, it represents appropriated parameter for the correlation see Figure 8.

Notice, that the undrained shear stiffness $|C_1P|$ is normalized by the mean stress p powered by $n = 0.75$. The coefficient n is observed within the limits defined by Viggiani & Atkinson (1995). Since the shear stiffness $|C_1P|$ is related to the normally consolidated soil it represents a reference value. The relation towards OCR was thus omitted.

It was observed that the specimens of low overconsolidation (OCR), in general reaches higher values of ν than their counterparts with higher OCR. Also, values of ν are generally lower (higher shear stiffness) for undisturbed specimens, indicating that ν which is to be used in finite element analyses of real case studies, should not be calibrated using shear experiments on reconstituted samples. This can be, however, partly be caused by the fact that reconstituted specimens are typically tested at lower OCRs than undisturbed specimens.

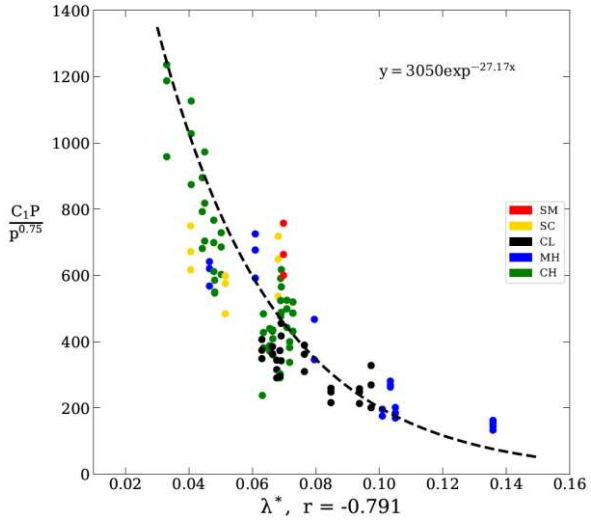

Figure 8: Correlation between λ^* and $\frac{C_1 P}{p^{0.75}}$

4.5 Summary of correlations

The correlations identified in this paper are summarised in Table 3 with their corresponding correlations coefficients.

Table 3: The summary of observed correlations

Equations	***Correlation Coefficient***
$\boldsymbol{N = 0.0118\, W_L + 0.4044}$	0.72
$\boldsymbol{N = 0.028\, W_L + 0.2429}$	0.88
$\boldsymbol{\lambda^* = 0.0849\, N - 0.0109}$	0.944
$\boldsymbol{\lambda^* = 0.001\, W_L - 0.0239}$	0.668
$\boldsymbol{\lambda^* = 0.0023\, W_P - 0.012}$	0.797
$\boldsymbol{\kappa^* = 0.278\, \lambda^* - 0.0074}$	0.854
$\boldsymbol{\kappa^* = 0.0238\, N - 0.0106}$	0.813
$\boldsymbol{\varphi_c = -0.233\, W_L + 38.46}$	-0.752
$\boldsymbol{\varphi_c = -0.402\, W_P + 37.9}$	-0.672

The correlations for the parameter λ^*, κ^* and N are derived from the $\ln(e+1) \times \ln p$ plane which is typical for the hypoplastic clay model. There correlations reach reasonable values. Although the correlations for φ_c agreed with the established knowledge, various relations between φ_c and soil properties can be found in the literature. However, it is found in this paper that parameter v does not show any strong relation to any other soil's properties such as grain size distribution or Atterberg's Limits. This parameter controls the model's shear stiffness, as illustrated with the response envelope. It is noted that the process in the previous section does not lead to accurate approximation of v, but rather an intepretation of the calibrated shear stiffness of the hypoplastic clay model.

5 CONCLUSIONS

This paper presents a study on the hypoplastic clay model parameters correlations with respect to other soil properties. The obtained correlations for N, λ^*, κ^* and φ_c are in a good agreement with existsing literature. Most of these correlations exhibits a satisfactory value of Pearson's coefficient (> 0.7), indicating their realiability and potential for further analysis.

The paper also provides a brief analysis of the parameter v. This parameter plays an important role in predicting stiffnesses of the hypoplastic model, and is dependent on the soil state. Although the parameters N, λ^*, κ^* and φ_c can be reasonably estimated from the derived relations, the parameter v should be determined based on the simulation of triaxial shear tests.

6 REFERENCES

Binod, T., Beena, A. 2011. A new correlation relating the shear strength of reconstituted soil to the proportions of clay minerals and plasticity characteristics, *Applied Clay Science* **53**, 48-57.

Gudehus, G., Mašín, D. 2009. Graphical representation of constitutive equations, *Géotechnique* **59**(2), 147-151.

Hong, Z. S., Zeng, L. L., Cui, Y. J., Cai, Y. Q., Lin, C. 2012. Compression behaviour of natural and reconstituted clays, *Géotechnique* **62**(4), 291-301.

Kadlíček, T., Janda, T., Šejnoha, M., Mašín, D., Najser, N., Beneš, Š. 2022a. Automated calibration of advanced soil constitutive models. Part I: Hypoplastic Sand, *Acta Geotechnica* **17**, 3421–3438.

Kadlíček, T., Janda, T., Šejnoha, M., Mašín, D., Najser, N., Beneš, Š. 2022b. Automated calibration of advanced soil constitutive models. Part II: hypoplastic clay and modified Cam-Clay, *Acta Geotechnica* **17**, 3439–3462.

Lupini, J. F., Skinner, A. E., Vaughan, P. R. 1981. The drained residual strength of cohesive soils, *Geotechnique* **31**(2), 181-213.

Mašín, D. 2013. Clay hypoplasticity with explicitly defined asymptotic states, *Acta Geotechnica,* **8**, 481–496.

Mašín, D. 2014. Clay hypoplasticity model including stiffness anisotropy. *Geotechnique* **64**(3), 232-238.

Schofield, A., Wroth, P. 1968. *Critical state soil mechanics,* London: Cambridge University.

Sharma, B., Bora, P. K. 2003. Plastic limit, liquid limit and undrained shear strength of soil reappraisal, *Journal of Geotechnical and Geoenvironmental engineering,* **129**(8), 774-777.

Viggiani, G., Atkinson, J. H. (1995). Stiffness of fine-grained soil at very small strains, *Géotechnique*, 249-265.

Wroth, C. a. (1978). The correlation of index properties with some basic engineering properties of soils, *Canadian Geotechnical Journal* **15**, 137-145.